Progress in higher order computations of prompt photon production in $e+A$ DIS at small x

Kaushik Roy,[ab] **Raju Venugopalan**[*b]

[a]*Department of Physics and Astronomy, Stony Brook University,*
Stony Brook, NY 11794, USA
[b]*Physics Department, Brookhaven National Laboratory,*
Bldg. 510A, Upton, NY 11973, USA

We compute the differential cross-section for inclusive prompt photon production in deeply in-elastic electron-nucleus scattering at small x in the framework of the Color Glass Condensate (CGC) effective field theory (EFT). At leading order in α_s, but all orders in Q_s^2/Q^2, where Q_s is the saturation scale in the nucleus, our result is proportional to universal dipole and quadrupole Wilson line correlators in the nucleus. Leading twist $k_\perp$ and collinearly factorized results are recovered in appropriate limits. We outline recent progress in extending the LO results to NLO+NLLx accuracy.

---

[*]Speaker.

1. Introduction

In the high energy "Regge-Gribov" limit of QCD, a semi-hard saturation scale $Q_s(x)$ emerges dynamically when repulsive gluon recombination and screening effects compete to tame the rapid growth in bremsstrahlung gluons with decreasing x. This novel saturation regime of QCD is described by a weak coupling effective field theory (EFT), the Color Glass Condensate (CGC) [1 – 7]. Isolated photons are clean probes of CGC because of the absence of final state interactions. CGC computations of inclusive photon production have been performed previously for a number of channels in $p + A$ collisions [8 – 11]. In this contribution, we will summarize the computation in [12], as well as work in progress, of the cross-section for inclusive prompt photon production in deeply inelastic scattering (DIS) of electrons off nuclei at small x.

Fig. 1 shows the two classes of leading order (LO) processes that are $O(\alpha_S^0)$ in the CGC power counting[1] The Class I diagram for photon bremsstrahlung is proportional to the valence quark distribution $f_q(x)$. At small x, since gluons play a dominant role, $f_g(x) \gg f_q(x)$, the Class II diagram shown dominates. This process can be visualized as the virtual photon fluctuating into a quark-antiquark dipole that subsequently emits a photon either before or after interacting with the target.
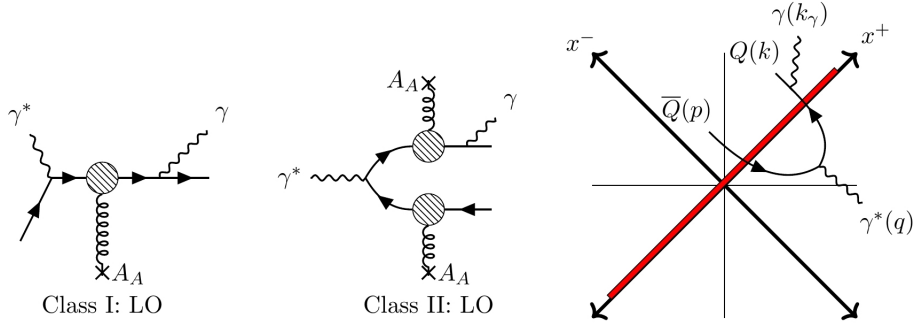

Class I: LO   Class II: LO

Figure 1: Representative Feynman diagrams for the LO processes at small x contributing to inclusive photon production. The blobs represent Wilson lines from the target that rotate the color charges of the quarks and antiquarks. The spacetime picture for the dominant Class II is also shown. The nucleus is considered to be right moving with $P_N^+ \to \infty$ and hence is Lorentz contracted in the x^- direction.

2. LO computation

In the CGC EFT, the abundant highly occupied small x gluons in the nuclear wave-function are described by solutions of the Yang-Mills equations:

$$[D_\mu, F^{\mu\nu}](x) = g\, \delta^{\nu+}\delta(x^-)\rho_A(\mathbf{x}_\perp). \tag{2.1}$$

---

[1]There is a third possible class in which photon is produced from quark-antiquark annihilation. Like its $p + A$ analog [9], this process is suppressed relative to those shown here.

1

The current induced by large x partons is described by a stochastic color charge density ρ_A. The momentum space dressed fermion propagator [3, 13, 14] in this background classical field computed in the Lorenz gauge $\partial_\mu A^\mu = 0$ is

$$S(p, p') = (2\pi)^4 \delta^{(4)}(p - p') S_0(p) + S_0(p) \, \mathscr{T}(p, p') \, S_0(p'), \tag{2.2}$$

where $S_0(p)$ is the free fermion propagator and the function $\mathscr{T}(p, p')$ represents the interaction vertex resumming all eikonal interactions ($O(g\rho_A \sim 1)$) with the nuclear "gluon shock wave" and is expressed as
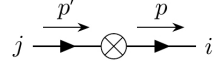

Figure 2: "Dressed" fermion propagator in the background classical color field of the nucleus. The $\otimes$ symbol denotes all multiple scattering insertions *including* as well, the possibility of no scattering. i and j denote color indices in the fundamental representation of $SU(N_c)$.

$$\mathscr{T}_{ij}(p, p') = (2\pi) \delta(p^- - p'^-) \gamma^- \mathrm{sign}(p^-) \int \mathrm{d}^2 \mathbf{z}_\perp e^{-i(\mathbf{p}_\perp - \mathbf{p}'_\perp) \cdot \mathbf{z}_\perp} \tilde{U}^{\mathrm{sign}(p^-)}_{ij}(\mathbf{z}_\perp), \tag{2.3}$$

where

$$\tilde{U}(\mathbf{x}_\perp) = \mathscr{P}_- \exp\left[-ig^2 \int_{-\infty}^{+\infty} \mathrm{d}z^- \frac{1}{\nabla^2_\perp} \rho^a_A(z^-, \mathbf{x}_\perp) t^a\right], \tag{2.4}$$

(see Fig. 2 for a diagrammatic representation of this propagator). This expression differs from those in the literature because it includes the"no scattering" contribution within the interaction vertex itself. This slight modification significantly reduces the number of diagrams at LO and is especially efficient in computing interactions with the shock wave at higher orders. Note that one must finally subtract the no scattering contribution (by setting $\tilde{U} = \mathbb{1}$) to obtain the physical scattering amplitude.

Our final expression for the LO amplitude is [12]

$$\mathscr{M}_{\mu\alpha}(\mathbf{q}, \mathbf{k}, \mathbf{p}, \mathbf{k}_\gamma) = 2\pi(eq_f)^2 \delta(P^- - q^-) \int_{\mathbf{x}_\perp, \mathbf{y}_\perp} \int_{\mathbf{l}_\perp} e^{-i\mathbf{P}_\perp \cdot \mathbf{x}_\perp + i\mathbf{l}_\perp \cdot \mathbf{x}_\perp - i\mathbf{l}_\perp \cdot \mathbf{y}_\perp}$$
$$\times \bar{u}(\mathbf{k}) \left[T^{(q\bar{q})}_{\mu\alpha}(\mathbf{l}_\perp, \mathbf{P}_\perp) \left[\tilde{U}(\mathbf{x}_\perp) \tilde{U}^\dagger(\mathbf{y}_\perp) - 1 \right] \right] v(\mathbf{p}). \tag{2.5}$$

In the above equation, $\mathbf{P}_\perp = \mathbf{k}_\perp + \mathbf{p}_\perp + \mathbf{k}_{\gamma\perp}$ and the explicit expression for $T^{(q\bar{q})}_{\mu\alpha}(\mathbf{l}_\perp, \mathbf{P}_\perp)$ can be found in [12]. We have verified that the amplitude in Eq. 2.5 satisfies the photon Ward identity. Additionally, by taking the soft photon limit $k_\gamma \to 0$, one recovers the non-radiative amplitude [15] for fully inclusive DIS which is a manifestation of the Low-Burnett-Kroll theorem [16 – 18]. This also allows us to reproduce extant results [19] of the differential cross-section for fully inclusive DIS dijet production.

Using the expression in Eq. 2.5, the triple differential cross-section for production of an isolated photon in association with 2 jets or a quarkonium state [12] is

$$\frac{\mathrm{d}\sigma}{\mathrm{d}x \mathrm{d}Q^2 \mathrm{d}^6 K_\perp \mathrm{d}^3 \eta_K} = \frac{\alpha^2 q_f^4 y^2 N_c}{512\pi^5 Q^2} (2\pi) \delta(P^- - q^-) \frac{1}{(2\pi)^4} \frac{1}{2q^-} L^{\mu\nu} \widetilde{X}_{\mu\nu}, \tag{2.6}$$

where $L^{\mu\nu}$ is the familiar lepton tensor in DIS and the hadron tensor is given by

$$\widetilde{X}_{\mu\nu} = \int_{l_{1\perp}} \int_{l_\perp, l'_\perp} (2\pi)^2 \delta^{(2)}(\boldsymbol{P}_\perp - \boldsymbol{l}_{1\perp}) \tau_{\mu\nu}{}^{q\bar{q},q\bar{q}}(\boldsymbol{l}_\perp, \boldsymbol{l}'_\perp | \boldsymbol{l}_{1\perp}) \times \left[\phi_0 - \frac{2\alpha_S}{N_c \boldsymbol{l}_{1\perp}^2} \Big(\phi_{Y_A}^D(\boldsymbol{l}_{1\perp} - \boldsymbol{l}_\perp, \boldsymbol{l}_\perp) \right.$$
$$\left. + \phi_{Y_A}^{D'}(\boldsymbol{l}_{1\perp} - \boldsymbol{l}'_\perp, \boldsymbol{l}'_\perp) + \phi_{Y_A}^Q(\boldsymbol{l}_{1\perp} - \boldsymbol{l}_\perp, \boldsymbol{l}_\perp; \boldsymbol{l}_{1\perp} - \boldsymbol{l}'_\perp, \boldsymbol{l}'_\perp) \Big) \right]. \tag{2.7}$$

Here $\tau_{\mu\nu}{}^{q\bar{q},q\bar{q}}$ is a Dirac trace [12]. The two nuclear unintegrated distributions $\phi_{Y_A}^D$ and $\phi_{Y_A}^Q$ are Fourier transforms of dipole and quadrupole Wilson line correlators in the nucleus. These are universal, gauge invariant quantities that are ubiquitous in high energy collisions. The expression for single inclusive photon production is obtained by integrating over the phase space for the quark and antiquark in Eq. 2.6.

We next consider the large transverse momentum limit of these unintegrated nuclear distributions and obtain the leading twist ($O(\rho_A)$) expression for Eq. 2.7. We have shown that this $k_\perp$-factorized photon production result can also be obtained through a pQCD analysis. The leading twist amplitude satisfies the gluon Ward identity [20, 10, 12] which leads to a well defined $\boldsymbol{P}_\perp \to 0$ limit for the collinearly factorized result for the hadron tensor [12]

$$\widetilde{X}_{\mu\nu}^{\text{coll.}} = \frac{2\alpha_S \pi^2}{N_c} \, (2\pi)^2 \delta^{(2)}(\boldsymbol{p}_\perp + \boldsymbol{k}_\perp + \boldsymbol{k}_{\gamma\perp}) \, x_A f_{g,A}(x_A, Q^2) \lim_{\boldsymbol{P}_\perp \to 0} \frac{\Theta_{\mu\nu}(\boldsymbol{P}_\perp)}{\boldsymbol{P}_\perp^2}. \tag{2.8}$$

We have thereby, in our framework, derived a clean relation between the inclusive photon spectrum and the nuclear gluon distribution at small x. Our result corresponds to the dominant contribution [21 – 24] at NLO($O(\alpha_S)$) in the pQCD power counting.

3. Structure and organization of the NLO computation

For precision computations in the gluon saturation regime, we need to extend our calculation to NLO accuracy. In the CGC power counting, this is equivalent to having external gluon lines and internal gluon loops that are not connected to the effective vertices (shockwave) in the Feynman diagrams. An essential component in this computation is the "shock wave" gluon propagator in an appropriate choice of gauge. We will work in the $A^- = 0$ gauge, which we shall refer to as the "wrong" light cone (LC) gauge[2] for the kinematics of our problem. The background field gluon propagator (see Fig. 3) in this gauge has a similar momentum space expression as Eq. 2.2 and the

Figure 3: Dressed gluon propagator with the dot representing the eikonal interaction vertex with the background classical field. This includes all possible scatterings including the case of "no scattering".

---

effective vertex is given by [3, 14, 12]

$$\mathcal{T}_{\mu\nu;ab}(p,p') = -2\pi\delta(p^- - p'^-) \times (2p^-)g_{\mu\nu} \ \text{sign}(p^-) \int d^2\mathbf{z}_\perp e^{-i(\mathbf{p}_\perp - \mathbf{p}'_\perp).\mathbf{z}_\perp} U_{ab}^{\text{sign}(p^-)}(\mathbf{z}_\perp),$$

(3.1)

where U is the Wilson line in Eq. 2.4 written in adjoint representation. The structures of the fermion and gluon effective vertices given by Eqs. 2.3 and 3.1 are respectively identical to the quark-quark-reggeon and gluon-gluon-reggeon vertices [25 – 28] in Lipatov's reggeon field theory [29].

In addition to the simple structure of the "shock wave" propagators in $A^- = 0$ gauge, we will also exploit the simplicity brought about by the natural separation between large x sources and small x "wee" partons that is ingrained in the CGC EFT (See Fig. 4).
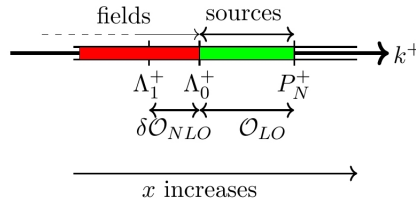

Figure 4: Schematic illustration of sources and fields in the CGC EFT. With high energy evolution, gluon field modes that were fields at higher x start qualifying as sources for the fields at smaller x.

At LO, this separation is arbitrary and the effects of the large x modes are included in a weight functional $W[\rho_A]$ describing the probability density of having a source configuration with charge density ρ_A. In our computation, this is inherent in the definitions of the different ϕ's that appear in Eq. 2.7. As we evolve towards the small x scale of interest, field modes that were below this cutoff start contributing to the scattering process. We therefore have to consider quantum effects due to the gluon modes with energies in the strip $\Lambda_0^- \ll |l^-| \ll \Lambda_1^- (= \Lambda_0^-/b)$ where $b \ll 1$ but $\alpha_S \ln(1/b) < 1$ so that a perturbative treatment of the logarithmic corrections is still possible. The rapidity separation between these "semi-fast" gluons leads to the occurence of the $\ln(\Lambda_1^-/\Lambda_0^-)$ log which, for $\alpha_S \ln(\Lambda_1^-/\Lambda_0^-) \sim 1$, changes the naive CGC power counting necessitating resummation of these logs to all orders.

In addition to parton subprocesses building up the nuclear shockwave, we also have gluon loop processes within the quark-antiquark dipole which suffer instantaneous interactions with the shockwave. These can be categorized broadly into real and virtual graphs. The latter is further subdivided into vertex and self-energy corrections. Due to the presence of the photon in the final state, we have a multitude of kinematically allowed contributions. Nevertheless, they can be systematically organized into a basis of dipole and quadrupole Wilson line correlators, and their products, or equivalently, in terms of the functions ϕ^D, ϕ^Q, $\phi^D\phi^D$ and $\phi^D\phi^Q$.

A distinctive feature of these Feynman graphs, characteristic of CGC computations, is that the gluon (both real and virtual) has the possibility of rescattering with the background classical field. For the emission of a real gluon, these transverse momentum kicks destroy the possibility of collinearity with the parent quark/antiquark; the UV divergent structure however remains unchanged under this effect in virtual graphs. The latter kind of divergences appear in the transverse

momentum integrations and will be regulated by dimensional regularization in $d = 2 - \varepsilon$ dimensions. However, a real gluon can also be emitted after the dipole crosses the "shock wave" in which case there are indeed collinear divergences. These will cancel exactly between real and virtual graphs. In addition, we get logarithms in rapidity (or $\ln(q^-/\Lambda_0^-)$) from integration over longitudinal momentum of the gluon when we regulate the spurious $l^- = 0$ pole in the free gluon propagator in $A^- = 0$ gauge by imposing a lower cutoff equal to Λ_0^- [30, 31].

The large logarithmic pieces accompanying the contributions discussed over the previous paragraphs can be absorbed in the weight functional describing the stochastic color cources. High energy evolution is then described as an evolution of these $W[\rho_A]$'s and forms the basis for non-linear evolution as described by the JIMWLK equation [32, 33, 30, 34, 35]. This procedure therefore allows us to factorize the cross-section into an "impact factor" contribution (free of rapidity logarithms) that is convoluted with generalized unintegrated nuclear distributions that have the RG evolution of the weight functional embedded in them.

Since we are also recovering the genuine α_S suppressed contributions or the NLO inclusive photon impact factor in this process, we can work one step further and mould existing results [36 – 41] on NLO($O(\alpha_S^2)$) BK and JIMWLK evolution into our RG framework to extend the results to NLO+NLLx accuracy. This can be achieved by collecting the $\alpha_S^2 \ln(\Lambda_1^-/\Lambda_0^-)$ pieces from the NLO evolution contributions and systematically combining them with LO(+LLx) and NLO impact factor results. We do not need to compute the finite pieces in the NLO JIMWLK contributions because they are formally next-to-next-to-leading order (NNLO) $O(\alpha_S^2)$ in the CGC power counting and hence suppressed at the required accuracy of our problem. This procedure is outlined in [12] and will be discussed at length along with presentation of the non-trivial NLO impact factor calculation in future work [42].

4. Conclusion

We outlined here the computation of the differential cross-section for inclusive photon production (Eq. 2.6) in small x DIS in the framework of CGC EFT. The result is sensitive to the physics of strongly correlated gluons in the saturation regime through its dependence on the universal multigluon Wilson line correlators in the nucleus. We discussed the ingredients, in particular the simple momentum space structures of the dressed quark and gluon propagators in the "wrong" LC gauge, that allow for efficient higher order computations. We sketched the Wilsonian RG ideology that will be adopted towards an extension of our results to NLO+NLLx accuracy; the non-trivial NLO impact factor computation [42] is nearing completion and will be presented soon. This work complements similar small x computations for fully inclusive [43 – 48] and diffractive DIS [49, 50] computations. They also provide useful insight into similar higher order computations in hadron-hadron collisions. From a phenomenological standpoint, isolated photon production at small x can be measured at the anticipated luminosities of a future Electron Ion Collider (EIC) [51] or LHeC [52]; the process is free of hadronization uncertainties and is therefore a golden probe of the structure of QCD matter at extreme gluon densities.

Acknowledgments

References

[1] L. D. McLerran and R. Venugopalan, *Computing quark and gluon distribution functions for very large nuclei*, *Phys. Rev.* **D49** (1994) 2233 [`hep-ph/9309289`].

[2] L. D. McLerran and R. Venugopalan, *Gluon distribution functions for very large nuclei at small transverse momentum*, *Phys. Rev.* **D49** (1994) 3352 [`hep-ph/9311205`].

[3] L. D. McLerran and R. Venugopalan, *Green's functions in the color field of a large nucleus*, *Phys. Rev.* **D50** (1994) 2225 [`hep-ph/9402335`].

[4] E. Iancu and R. Venugopalan, *The Color glass condensate and high-energy scattering in QCD*, in *In *Hwa, R.C. (ed.) et al.: Quark gluon plasma* 249-3363*. 2003. `hep-ph/0303204`. DOI.

[5] F. Gelis, E. Iancu, J. Jalilian-Marian and R. Venugopalan, *The Color Glass Condensate*, *Ann. Rev. Nucl. Part. Sci.* **60** (2010) 463 [`1002.0333`].

[6] Y. V. Kovchegov and E. Levin, *Quantum chromodynamics at high energy*, vol. 33. Cambridge University Press, 2012.

[7] J.-P. Blaizot, *High gluon densities in heavy ion collisions*, *Rept. Prog. Phys.* **80** (2017) 032301 [`1607.04448`].

[8] F. Gelis and J. Jalilian-Marian, *Photon production in high-energy proton nucleus collisions*, *Phys. Rev.* **D66** (2002) 014021 [`hep-ph/0205037`].

[9] S. Benic and K. Fukushima, *Photon from the annihilation process with CGC in the pA collision*, *Nucl. Phys.* **A958** (2017) 1 [`1602.01989`].

[10] S. Benic, K. Fukushima, O. Garcia-Montero and R. Venugopalan, *Probing gluon saturation with next-to-leading order photon production at central rapidities in proton-nucleus collisions*, *JHEP* **01** (2017) 115 [`1609.09424`].

[11] S. Benić, K. Fukushima, O. Garcia-Montero and R. Venugopalan, *Constraining unintegrated gluon distributions from inclusive photon production in proton-proton collisions at the LHC*, `1807.03806`.

[12] K. Roy and R. Venugopalan, *Inclusive prompt photon production in electron-nucleus scattering at small x*, *JHEP* **05** (2018) 013 [`1802.09550`].

[13] L. D. McLerran and R. Venugopalan, *Fock space distributions, structure functions, higher twists and small x*, *Phys. Rev.* **D59** (1999) 094002 [`hep-ph/9809427`].

[14] I. I. Balitsky and A. V. Belitsky, *Nonlinear evolution in high density QCD*, *Nucl. Phys.* **B629** (2002) 290 [`hep-ph/0110158`].

[15] F. Gelis and J. Jalilian-Marian, *From DIS to proton nucleus collisions in the color glass condensate model*, *Phys. Rev.* **D67** (2003) 074019 [`hep-ph/0211363`].

[16] F. E. Low, *Bremsstrahlung of very low-energy quanta in elementary particle collisions*, *Phys. Rev.* **110** (1958) 974.

[17] T. H. Burnett and N. M. Kroll, *Extension of the low soft photon theorem*, *Phys. Rev. Lett.* **20** (1968) 86.

[18] J. S. Bell and R. Van Royen, *On the low-burnett-kroll theorem for soft-photon emission*, *Nuovo Cim.* **A60** (1969) 62.

[19] F. Dominguez, C. Marquet, B.-W. Xiao and F. Yuan, *Universality of Unintegrated Gluon Distributions at small x*, *Phys. Rev.* **D83** (2011) 105005 [`1101.0715`].

[20] F. Gelis and R. Venugopalan, *Large mass qq̄ production from the color glass condensate*, *Phys. Rev.* **D69** (2004) 014019 [`hep-ph/0310090`].

[21] P. Aurenche, A. Douiri, R. Baier, M. Fontannaz and D. Schiff, *The Deep Compton Scattering: Single Photon Spectrum and Photon - Hadron Correlations Beyond Leading Logarithms*, *Z. Phys.* **C24** (1984) 309.

[22] A. Gehrmann-De Ridder, G. Kramer and H. Spiesberger, *Photon plus jet-cross sections in deep inelastic e p collisions at order O(alpha**2 alpha(s))*, *Nucl. Phys.* **B578** (2000) 326 [`hep-ph/0003082`].

[23] G. Kramer, D. Michelsen and H. Spiesberger, *Production of hard photons and jets in deep inelastic lepton proton scattering at order O (alpha-s)*, *Eur. Phys. J.* **C5** (1998) 293 [`hep-ph/9712309`].

[24] D. Michelsen, *Radiative corrections of order alpha-s for production of hard photons by HERA*, Ph.D. thesis, Hamburg U., 1995.

[25] S. Bondarenko, L. Lipatov, S. Pozdnyakov and A. Prygarin, *One loop light-cone QCD, effective action for reggeized gluons and QCD RFT calculus*, *Eur. Phys. J.* **C77** (2017) 630 [`1708.05183`].

[26] M. Hentschinski, *The Color Glass Condensate formalism, Balitsky-JIMWLK evolution and Lipatov's high energy effective action*, `1802.06755`.

[27] S. Bondarenko and S. Pozdnyakov, *S-matrix and productions amplitudes in high energy QCD*, `1803.04131`.

[28] S. Bondarenko and S. Pozdnyakov, *On correlators of Reggeon fields and operators of Wilson lines in high energy QCD*, `1806.02563`.

[29] L. N. Lipatov, *Small x physics in perturbative QCD*, *Phys. Rept.* **286** (1997) 131 [`hep-ph/9610276`].

[30] E. Iancu, A. Leonidov and L. D. McLerran, *Nonlinear gluon evolution in the color glass condensate. 1.*, *Nucl. Phys.* **A692** (2001) 583 [`hep-ph/0011241`].

[31] G. Beuf, *Improving the kinematics for low-x QCD evolution equations in coordinate space*, *Phys. Rev.* **D89** (2014) 074039 [`1401.0313`].

[32] J. Jalilian-Marian, A. Kovner, A. Leonidov and H. Weigert, *The BFKL equation from the Wilson renormalization group*, *Nucl. Phys.* **B504** (1997) 415 [`hep-ph/9701284`].

[33] J. Jalilian-Marian, A. Kovner and H. Weigert, *The Wilson renormalization group for low x physics: Gluon evolution at finite parton density*, *Phys. Rev.* **D59** (1998) 014015 [`hep-ph/9709432`].

[34] E. Iancu, A. Leonidov and L. D. McLerran, *The Renormalization group equation for the color glass condensate*, *Phys. Lett.* **B510** (2001) 133 [`hep-ph/0102009`].

7

[35] E. Ferreiro, E. Iancu, A. Leonidov and L. McLerran, *Nonlinear gluon evolution in the color glass condensate. 2.*, *Nucl. Phys.* **A703** (2002) 489 [`hep-ph/0109115`].

[36] I. Balitsky and G. A. Chirilli, *Rapidity evolution of Wilson lines at the next-to-leading order*, *Phys. Rev.* **D88** (2013) 111501 [`1309.7644`].

[37] I. Balitsky and G. A. Chirilli, *Next-to-leading order evolution of color dipoles*, *Phys. Rev.* **D77** (2008) 014019 [`0710.4330`].

[38] A. V. Grabovsky, *Connected contribution to the kernel of the evolution equation for 3-quark Wilson loop operator*, *JHEP* **09** (2013) 141 [`1307.5414`].

[39] A. Kovner, M. Lublinsky and Y. Mulian, *Jalilian-Marian, Iancu, McLerran, Weigert, Leonidov, Kovner evolution at next to leading order*, *Phys. Rev.* **D89** (2014) 061704 [`1310.0378`].

[40] M. Lublinsky and Y. Mulian, *High Energy QCD at NLO: from light-cone wave function to JIMWLK evolution*, *JHEP* **05** (2017) 097 [`1610.03453`].

[41] S. Caron-Huot, *When does the gluon reggeize?*, *JHEP* **05** (2015) 093 [`1309.6521`].

[42] K. Roy and R. Venugopalan *in preparation* .

[43] I. Balitsky and G. A. Chirilli, *Photon impact factor in the next-to-leading order*, *Phys. Rev.* **D83** (2011) 031502 [`1009.4729`].

[44] I. Balitsky and G. A. Chirilli, *Photon impact factor and k_T-factorization for DIS in the next-to-leading order*, *Phys. Rev.* **D87** (2013) 014013 [`1207.3844`].

[45] G. Beuf, *NLO corrections for the dipole factorization of DIS structure functions at low x*, *Phys. Rev.* **D85** (2012) 034039 [`1112.4501`].

[46] G. Beuf, *Dipole factorization for DIS at NLO: Loop correction to the $\gamma_{T,L}^* \to q\bar{q}$ light-front wave functions*, *Phys. Rev.* **D94** (2016) 054016 [`1606.00777`].

[47] G. Beuf, *Dipole factorization for DIS at NLO: Combining the $q\bar{q}$ and $q\bar{q}g$ contributions*, *Phys. Rev.* **D96** (2017) 074033 [`1708.06557`].

[48] B. Ducloue, H. Hanninen, T. Lappi and Y. Zhu, *Deep inelastic scattering in the dipole picture at next-to-leading order*, *Phys. Rev.* **D96** (2017) 094017 [`1708.07328`].

[49] R. Boussarie, A. V. Grabovsky, L. Szymanowski and S. Wallon, *Impact factor for high-energy two and three jets diffractive production*, *JHEP* **09** (2014) 026 [`1405.7676`].

[50] R. Boussarie, A. V. Grabovsky, L. Szymanowski and S. Wallon, *On the one loop $\gamma^{(*)} \to q\bar{q}$ impact factor and the exclusive diffractive cross sections for the production of two or three jets*, *JHEP* **11** (2016) 149 [`1606.00419`].

[51] A. Accardi et al., *Electron Ion Collider: The Next QCD Frontier*, *Eur. Phys. J.* **A52** (2016) 268 [`1212.1701`].

[52] LHeC Study Group collaboration, J. L. Abelleira Fernandez et al., *A Large Hadron Electron Collider at CERN: Report on the Physics and Design Concepts for Machine and Detector*, *J. Phys.* **G39** (2012) 075001 [`1206.2913`].